Sawtooth-free Ohmic Discharges in ASDEX and the Aspects of Neoclassical Ion Transport

U. Stroth

IPP III / 178

MAY 1991

MAX-PLANCK-INSTITUT FÜR PLASMAPHYSIK

8046 GARCHING BEI MÜNCHEN

MAX-PLANCK-INSTITUT FÜR PLASMAPHYSIK
GARCHING BEI MÜNCHEN

Sawtooth-free Ohmic Discharges in ASDEX and the Aspects of Neoclassical Ion Transport

U. Stroth

IPP III / 178

MAY 1991

Die nachstehende Arbeit wurde im Rahmen des Vertrages zwischen dem Max-Planck-Institut für Plasmaphysik und der Europäischen Atomgemeinschaft über die Zusammenarbeit auf dem Gebiete der Plasmaphysik durchgeführt.

SAWTOOTH-FREE OHMIC DISCHARGES IN ASDEX AND THE ASPECTS OF NEOCLASSICAL ION TRANSPORT

U. Stroth, G. Fußmann, K. Krieger, V. Mertens, F. Wagner,
M. Bessenrodt-Weberpals, R. Büchse, L. Giannone,
H. Herrmann, E. Simmet, K.-H. Steuer
and the ASDEX Team

Max-Planck-Institut für Plasmaphysik,
EURATOM-IPP Association D-8046 Garching, FRG

Sawtooth-free Ohmic discharges can serve as a model case for a quiescent Tokamak plasma. We report on the properties and the global parameters of these discharges observed in ASDEX and make comments on the mechanism which seems to be responsible for the stabilization of the sawtooth instability. Stationary Ohmic discharges were used to investigate particle, impurity and energy transport in the absence of the sawtooth instability. Particular emphasis has been devoted to a comparison with the predictions of neoclassical theories. We find that the ion energy transport is on the level predicted by neoclassical theory and can explain particle and impurity transport with neoclassical inward drift velocities and diffusion coefficients with the same small anomalous contribution. In the central region of the plasma, were the power flux is low, very small values were found for the electron heat conductivity.

1. Introduction

Tokamak plasma discharges with radially peaked density profiles are known to have improved energy and particle confinement properties. The positive effect of a peaked density profile on confinement has been demonstrated in Ohmically and neutral beam injection (NI) heated plasmas. At ASDEX the Improved Ohmic Confinement (IOC) regime [1], pellet [2] and counter neutral beam injection discharges [3] belong to this type of plasma. The physical processes leading to the density profile peaking may be different in the various regimes and are not yet entirely understood.

As found in other regimes of improved energy confinement, discharges with peaked density profiles suffer from impurity accumulation, which always goes along with an improvement in particle confinement. Hence, what is gained in β by improving the energy confinement is partly lost by a higher impurity radiation level. In these cases quasi stationary conditions can only be reached if sawtooth activity limits the central impurity concentration. In the H-mode, ELMs eject impurities from the plasma edge. In counter NI heated discharges where the sputtering of impurities and therefore the impurity flux into the plasma is high neither sawteeth nor ELMs are present and accumulation of impurities leads to disruptions.

In contrast to the H-mode, where for ASDEX improved energy confinement has been attributed to a reduction in the electron energy transport [4], in plasmas with peaked density profiles a reduction of the transport in the ion channel seems to be the reason of the global improvement in confinement [5,6]. Detailed transport calculations are, however, difficult to perform since, as previously discussed, most of these discharges do not have stationary phases or are, as pellet fuelled or IOC plasmas, at high densities where electron and ion energy transport channels are difficult to separate.

Recently, sawtooth-free Ohmic discharges have been investigated on ASDEX. They also belong to the class of discharges with peaked density profiles. Since they achieve stationarity with a saturation in the central impurity concentration they can be used as model discharges for the investigation of the physics of tokamak plasmas with peaked density profiles. The low to moderate line averaged density of these discharges allows for a separation of electron and ion energy transport. Furthermore, with respect to particle and impurity transport, these quiescent plasmas can be used to study the intrinsic transport processes undisturbed from the usually superimposed sawtooth activities.

Sawtooth-free discharges have already been investigated in other tokamaks. In Pulsator, transitions to sawtooth-free phases could appear in discharges with steadily increasing density leading to disruptions below the density limit [16]. In JET sawtooth-free phases occur in combined ICRH and NI heated discharges [7] and were used for local transport studies [8]. In Doublet III, Ohmic sawtooth-free plasmas were named O-type discharges. They show similar characteristics as the discharges reported here but stationary discharges could not be established [9].

The paper is organized as follows: We first describe the characteristics of sawtooth-free discharges and their global parameters. Thereafter we discuss the mechanism stabilizing the sawteeth. Finally, particle, impurity and energy transport found in quiescent

sawtooth-free discharges are analysed.

2. Properties of Sawtooth-Free Discharges

In this section we summarize the global properties of sawtooth-free discharges and how they have been achieved in ASDEX.

The systematic investigation of sawtooth-free discharges has become possible after carbonization [10] or boronization of the ASDEX vacuum vessel [11]. They appear in a transition stage from freshly boronized to unboronized conditions. This gives reason to the assumption that sawtooth-free plasmas need a specific impurity mixture to develop. Only under these conditions sawtooth-free phases can be reached as soon as the external gas flux to the plasma is reduced so that a density plateau at a low line averaged density is established. The exact prerequisites for sawtooth-free discharges could not be identified unambiguously. It is interesting, however, that sawtooth-free discharges could be obtained under machine conditions which were not favourable for the achievement of the IOC regime. But both regimes are triggered by the shut off of the gas valve.

As an example, in Fig. 1 we compare the temporal evolution of discharges with and without sawteeth. The discharges have identical plasma control parameters. The small difference of the discharges in toroidal field strength (B_t) is not responsible for the different behaviour since sawtooth-free discharges could be produced in a wide range of B_t values (see also Fig. 14,15). The bifurcation appears at 0.5 s. A small extra gas puff from the feed-back system (see arrow in Fig. 1) broadens the density profile of one of the discharges as it can be seen at the density peaking factor (central to volume averaged electron density, $Q_N = n_e(0)/\bar{n}_e^V$). For this discharge the sawteeth develop as usual. When the plateau density is reached, the external gas flux is reduced. This leads to a strong density profile peaking in the other discharge while the already sawtoothing one does not change its density profile. The discharge with the peaked density profile stays sawtooth-free throughout the first Ohmic phase which ends with NI at 1 s.

The peaking of the density profile induces impurity accumulation. Without provoking a disruption, the accumulation is saturated prior to the NI-pulse, as it can be seen from the soft X-ray signal. In the early injection phase the still Ohmic confinement properties and a central beam particle deposition lead to a further peaking of the density profile. Thereafter, the confinement changes to L-mode properties. The particle confinement time is decreased and the external gas flux has to be enhanced in order to maintain the pre-programmed line averaged density. As a consequence the density profile starts to flatten and a reduction of the impurity radiation takes place. The onset of the sawteeth occurs when the density profile has flattened and Q_N is approaching the level of discharges with sawteeth. Only after the first sawtooth, the impurity radiation drops to the level of the other discharge with sawteeth.

We conclude that Ohmic discharges at low densities can exist in two different plasma configurations with the same external parameters. The density profile is either peaked when the sawteeth are absent or flat when they are present. Density profiles in between these limits cannot be realized under equilibrium conditions.

As illustrated in Fig. 2, the strong peaking in the initial phase of the sawtooth-free discharge in Fig. 1 is a process bound to the plasma centre leaving the outer half of the cross-section unchanged. The density profiles are drawn as fits to the data of our multiple Thomson scattering system [12]. They represent profiles before, during and after the strong rise in Q_N seen in Fig. 1 around 0.7 s. The change in the density profile occurs for $r \leq 15$ cm; further out the profiles coincide within the error bars of the data. In contrast to Doublet III [9], we do not observe broader electron temperature profiles in the early stage of sawtooth-free discharges than for discharges with sawteeth.

In Figs. 3 and 4 we summarize the influence of the sawteeth on the density and temperature profile shapes. The figures refer to low density Ohmic deuterium plasmas ($\bar{n}_e \leq 3 \times 10^{19}\mathrm{m}^{-3}$). The effect of a distinct gap between the density peaking of the discharges with and without sawteeth in Fig. 1 can also be seen in Fig. 3. The size of the gap depends on the edge safety factor q_a. The density peaking of sawtooth-free discharges does not depend on q_a and is between 2.1 and 2.3. Conversely, the peaking of the density profile of discharges with sawteeth increases with q_a as expected from the reduction of the sawtooth extension with the shrinking q=1 surface. Q_N is 1.5 at low q_a and 1.8 at q_a=4.3. Asymptotically, as the q=1 surface vanishes, Q_N appears to converge to the value of the sawtooth-free discharges. For $q_a > 5$, sawteeth do no longer develop.

The effect of sawteeth on the density profile can be estimated by the following consideration: Assuming that the sawtooth activity basically flattens the density profile inside the q=1 surface one can calculate from a peaked density profile the peaking of the corresponding profile with sawteeth via a definition of an equivalent density peaking factor $\tilde{Q}_N = n_e(r_{q=1})/\bar{n}_e^V$. The q=1 radius is taken from the relation $r_{q=1} = a/q_a$, observed in ASDEX for discharges with sawteeth. With this definition one calculates from the density profiles shown in Fig. 14 values which fit well to the results for discharges with sawteeth in Fig. 3: $\tilde{Q}_N$=1.53, 1.62 and 1.7 for q_a=3, 3.3 and 3.6, respectively.

This comparison reinforces the view that the peaked and q-independent density profiles of sawtooth-free discharges are actually the canonical density profiles of a stable plasma. What is seen normally is a deviation from it on account of sawtooth activity.

The density peaking factor is the same in sawtooth-free helium and deuterium discharges. In pure hydrogen plasmas sawtooth-free phases could not be established.

The peaking of the radial electron temperature (T_e) profile depends on q_a irrespective whether the discharges have sawteeth or not (see Fig. 4). With decreasing q_a the temperature profile flattens in both cases. In the sawtoothing discharges this occurs because of an expanding q=1 at identical sawtooth period and a consequent enhancement of the sawtooth energy transport. In the sawtooth-free discharges the impurity accumulation levels off at values the higher the lower q_a is. The role of the electron energy transport coefficients will be discussed later.

In order to reach high densities stronger external gas puffing is necessary and sawtooth-free discharges are more difficult to achieve. For this reason our investigations are restricted to the low density domain ($n_e \leq 3 \times 10^{19}\mathrm{m}^{-3}$). We observed, however, two sawtooth-free discharges during a density limit program. These discharges remained sawtooth-free from the beginning up to the density limit at the high line averaged value

of $7 \times 10^{19}\mathrm{m}^{-3}$. This has to be compared with a density limit of $6.4 \times 10^{19}\mathrm{m}^{-3}$ in the corresponding sawtoothing discharge (at I_P=320 kA and B_t=2.17 T). For these discharges it has not been attempted to establish a density plateau; the ramping rate was $3{\times}10^{19}$ $\mathrm{cm}^{-3}\mathrm{s}^{-1}$.

The cited high density discharges are included in Fig. 5 were the global energy confinement time τ_E is shown for discharges with and without sawteeth. In the Linear Ohmic Confinement regime (LOC) the energy confinement time of the sawtooth-free discharges is at the upper boundary of the values found for discharges with sawteeth. There is less scattering in the τ_E values for the discharges with sawteeth because they are taken from a data base with fixed q_a.

The values for the sawtooth-free discharge at higher density have to be taken with caution because they do not come from stationary phases. As it can be seen in Fig. 6, the density peaking is not fully developed because additional gas puffing is applied in order to increase the density further. But even so, the energy confinement time is superior to the values in the Saturated Ohmic Confinement regime (SOC). There is one point in Figs. 5 and 6 at the highest density which shows higher values for τ_E and Q_N. This point was taken at the end of the discharge, when the gas flux already had been shut off. It indicates that density peaking and confinement time might be superior to the values shown at high densities if they were obtained during stationary phases. It is not clear, however, whether they would reach the measured values of the IOC regime.

Even if the energy confinement time of sawtooth-free discharges at high densities was somewhat higher as shown in the figure, a striking feature would prevail, i.e. that τ_E does not seem to depend on the line averaged density. In taking the results of Fig. 6 into consideration a consistent picture emerges. For discharges with sawteeth, density peaking and confinement time are correlated, both increase in the LOC and IOC regimes with density and both saturate in the SOC regime. In sawtooth-free discharges no dependence of the density peaking factor on line averaged density is found. Consequently no dependence of τ_E on the density is observed. One would, however, expect the confinement time without sawteeth to be superior to the values in the IOC regime. This is in contradiction to the observations in Fig. 5. The picture does not change substantially if one plots the radiation corrected confinement times.

Recently, a comparison of SOC and IOC plasmas showed that these regimes are distinct in their edge plasma parameters [13]. A simple model, connecting power flux across the Scrape-Off Layer (SOL) to edge plasma parameters, has been confirmed by data from SOC and IOC plasmas: IOC discharges are characterized by lower power fluxes across the SOL and, according to the model, by lower edge density than the SOC discharges. The low edge density triggers a steepening of the density profile from the edge and an increase in Q_N. Contrarily, the sawtooth-free phases were achieved in clean plasmas with low impurity radiation losses and consequently high edge density values. The density peaking of these plasmas comes from the plasma centre and has therefore a very different origin.

From these considerations one can argue that density profiles can be radially peaked by two steps, (i) centrally by stabilization of the sawtooth activity and (ii) from the edge by

decreasing the power flux across the SOL. (i) is realized in sawtooth-free discharges and (ii) in IOC plasmas. A combination of both might be the origin of the strong peaking in pellet refuelled discharges where sawteeth are suppressed and edge fuelling substituted by bulk fuelling. An interpretation in this line is supported by the results given in Fig. 7. Pellet refuelled discharges have the steepest density profile gradient. Sawtooth-free and IOC discharges come in the centre and the edge, respectively, closest to these values. The broad density profile of an SOC plasma is comparable to IOC in the centre and to sawtooth-free discharges in the edge. The highest energy confinement times are indeed observed with pellet refuelling.

3. Sawtooth Stabilization

The sawtooth instability has a strong influence on the central plasma confinement. Especially during additional plasma heating it limits the central temperature and, ejecting energetic particles from the plasma centre, has a limiting effect on the heating efficiency. Although the suppression of sawteeth has the disadvantage of allowing impurity accumulation, the beneficial effect of reducing the transport can, however, result in a net improvement in confinement. This has been demonstrated in the IOC regime at ASDEX [1] where the sawtooth activity is reduced. Similarly, during sawtooth-free phases in combined ICRF and NI heated plasmas at JET an improvement of up to 20% in energy confinement time is found [7].

Two mechanisms can in principle stabilize the sawtooth instability: the vanishing of the q=1 surface with a central q value above 1 or stabilization of the m=1 mode growth by profile effects in the presence of a q=1 surface. (Stabilization by energetic ions does not play a role in the Ohmic plasmas of ASDEX.)

In ASDEX, counter NI and pellet refuelled discharges are alike [14] and follow the first mechanism mentioned above: A change in the particle transport behaviour and moderately peaked density profiles result in impurity accumulation in the plasma centre. This leads to an increasing central Z_{eff} and, because of high radiative losses, to a decreasing central electron temperature; the current profile broadens and the central q value rises above 1 [15]. The same mechanism might be the reason for the sawtooth-free phases reported for Pulsator [16].

By means of lower-hyprid current drive (LHCD) the current profile can be modified directly. Experiments at ASDEX have shown [17,18] that LHCD is able to broaden the current profile in a way that q is above 1 everywhere. In PLT [19] and, with a modified lower hybrid deposition profile, in ASDEX [20] it has been shown that sawtooth-free phases can coexist with an m=1 mode. In this case a centrally flat q profile with an off-axis minimum below 1 possibly explains the observations [21].

A stabilization of the sawtooth instability in the presence of a central q value below 1 occurs in some of the discharges which are investigated in this paper. This is demonstrated in Fig. 8. The upper part shows line averaged density ($\bar{n}_e$) and the soft X-ray intensity, integrated along a chord of 5 cm minor radius, of a sawtooth-free Ohmic discharge with I_P=250 kA and q_a=4.2. This discharge remained stable for 3 s while the

density has been ramped from a plateau at $\bar{n}_e = 2.1 \times 10^{19} \mathrm{m}^{-3}$ to $3.3 \times 10^{19} \mathrm{m}^{-3}$. During the first density plateau a strong m=1 mode reveals the presence of a q=1 surface. This is in accordance with neoclassical current density calculations which are shown in the lower left part of the Figure. The current profiles have been calculated using measured bremsstrahlung Z_{eff} and electron temperature profiles with neoclassical resistivity as published in Ref. [22]. The calculation gives a q=1 surface at $r \cong 9$ cm in accordance with the data from the soft X-ray camera array, where the m=1 activity vanishes between 7.5 and 10 cm. At 1 s the density is ramped up to a second plateau. At the higher density the T_e profile broadens. Consequently the current profile broadens too and the central q value increases above 1. This again agrees with the observation from the soft X-ray data, which shows that the m=1 mode vanishes. From this comparison we learn that neoclassically calculated current profiles compare well with information about the q profile which were obtained from soft X-ray measurements and that the sawtooth instability can be stabilized when the central q value obtained by these calculations is below 1. Using Spitzer resistivity yields flat q profiles for the sawtooth-free phase with values in the vicinity of 1 in the plasma centre.

Information regarding the crucial mechanism which leads to stabilization can be found from a discharge similar to the sawtooth-free one in Fig. 1, which has Ohmic phases with and without sawteeth. The electron temperature profiles in both phases are practically identical (see full lines in Fig. 15). The Z_{eff} profile is more peaked in the sawtooth-free phase but the central q ($q(0) \cong 0.77$) and the location of the q=1 surface ($r_{q=1} \cong 12$ cm) are only slightly different. This again follows from current density calculations which are based on sawtooth averaged profiles in the phase with sawteeth. The major difference in the two phases is in the density profiles in the plasma centre (see full lines in Fig. 14). The density gradient at the q=1 surface is by a factor of 2 higher in the sawtooth-free phase ($n_e'/n_e \mid_{q=1} = 4.4\ \mathrm{m}^{-1}$) than in the phase with sawteeth ($n_e'/n_e \mid_{q=1} = 2.3\ \mathrm{m}^{-1}$). Hence, the steep density gradient in the region of the q=1 surface might stabilize the sawteeth. This is also supported by theoretical investigations of Coppi et al. Ref [23].

Another hint that the density gradient might have a stabilizing effect on the sawtooth instability is given in the NI heated phase of the discharge in Fig. 1. At 1.2 s, the density profile starts to flatten. This happens without a sawtooth and the impurity radiation stays at a high level. Only 70 ms later,when the density profile has already lost its peakedness, sawteeth set in.

In the previous section we have seen, that the external gas flux can trigger a process which is peaking the density profile. The influence of the gas flux on the density profile and therefore on the sawtooth behaviour is the content of Fig. 9. An Ohmic discharge has been continuously ramped up in density. Then the gas valve has been shut off at 1.9 s and the line averaged density starts dropping while the heating power remains unchanged. From the edge a peaking of the density profile, shown in Q_N, is triggered and the sawtooth period increases from 15 to 21 ms. The sawtooth period does not only depend on line averaged density but also on other parameters which again depend on the external fuelling rate. The turning point in the diamagnetic beta poloidal (β_{pol}) is 100 ms later than in the density and, comparing times corresponding to the same line averaged density, a higher value for β_{pol} is found after the shut off of the gas valve, where the

density is more peaked. β_{pol} is not only a function of density: $\beta_{pol} = f(\bar{n}_e, Q_N)$. But Fig. 9 also shows that a strong density peaking does not necessarily lead to a stabilization of the sawtooth instability. There must be additional conditions which have to be fulfilled and an exact understanding of the processes involved remains elusive.
Also from JET the stabilization of the sawtooth instability in the presence of $q(0) \leq 1$ has been reported for the ICRH plasmas mentioned above. There the stabilization has been tentatively explained as being due to the fast ions which are produced by the ICRH [24]. This process can not be involved in the plasmas discussed here.

4. Transport

Energy, plasma particle and impurity transport from the plasma centre is dominated by the sawteeth. It is not justified to include sawtooth induced transport in the coefficients which drive the transport along the gradients of the equilibrium plasma profiles. Transport driven by sawteeth has to be explicitly added as a superimposed mechanism to the transport equations. Hence, experimental transport coefficients for the inner plasma regions are subject to large uncertainties. In particular, results on the q dependence of the transport coefficients must depend sensitively on the model used for the sawtooth induced transport.
Sawtooth-free discharges do not suffer from these problems. They are therefore best suited as representatives for the intrinsic transport coefficients of quiescent plasmas.

4.1. *Plasma Particle Transport*

The particle transport problem is usually solved in the form:

$$\Gamma_n(r) = 4\pi^2 R_0 \int_0^r \left(Q_{ion}(r') - Q_{rec}(r') - \frac{\partial n_e(r')}{\partial t} \right) r' dr', \quad (1)$$

$$\Gamma_n(r) = n_e(r) v_{in}(r) S(r) - D(r) \nabla n_e(r) S(r). \quad (2)$$

Here $\Gamma_n(r)$ is the net particle flux across the flux surface area $S(r)$ with the minor radius r. It is calculated from the neutral ionisation source Q_{ion}, the recombination loss Q_{rec} and the variation of the density profile with time. R_0 is the major plasma radius. From Eq. 1 one gets an experimental estimate of the net particle outward flux, which can by analysed with the help of Eq. 2 in terms of an inward drift velocity ($v_{in}(r)$) and a particle diffusion coefficient ($D(r)$). Analysing one density profile for a given time can only result in the evaluation of the quotient $v(r)/D(r)$. Often density profiles from different phases of a plasma discharge are taken to estimate, for example, $v(r)/D(r)$ from a stationary and the absolute values of the transport coefficients from a dynamic phase. Then, naturally, both quantities have to be assumed independent from the plasma parameters which might change from one phase to the other. Here we chose a different method. We use the neoclassical prediction for the inward drift velocity as found in Ref. [25] and calculate the particle diffusion coefficient as a function of radius from Eq. 2. In

OH discharges the particle inward flux is strong enough to account for the density built up which occurs after pellet injection [26] and after a sawtooth crash.
In Fig. 10 the particle diffusion coefficients for a sawtooth-free discharge and for a discharge with sawteeth, where the analyses are undertaken during a sawtooth rise, are compared. The inward drift is in both cases of the order of 0.25 m/s. The q=1 surface is r=9 cm in the sawtooth-free discharge (q_a=3.0) and r=12 cm in the other case (q_a=2.75). Only for the inner region of the plasma a substantial reduction of the diffusion coefficient is found when the sawteeth cease. The plasma centre of the discharge which has been analysed in between two successive sawtooth crashes seems to have some memory of the preceding event. But since the toroidal electric field in the plasma centre of a sawtoothing discharge might be different from the field which has been deduced from the measured loop voltage, the error bars on the neoclassical inward drift velocity can be large.
The same type of analyses has been carried out for sawtooth-free discharges at q_a values between 2.5 and 4.5. The results are given in Fig. 11; circles and squares represent discharges where the variation in q_a was realized at constant magnetic field strength and constant plasma current, respectively. For this Figure, the diffusion coefficient has been averaged between $a/4 \leq r \leq 3a/4$. The error bars represent the variation of D in this region. The two discharges from Fig. 10 are included in this Figure. We do not find a q_a dependence of the particle diffusion coefficient for sawtooth-free discharges. The average value of D in the region which excludes centre and plasma edge is of the order of 0.1 m^2/s for sawtooth-free discharges and a discharge with sawteeth. The neoclassical prediction for the particle diffusion coefficient is a factor of 50 smaller. Anomalous particle transport prevails in this zone.
A value of $D(r)$ ~0.1 m^2/s has also be found in ASDEX for Ohmic post pellet phases Ref. [26]. These analyses have been carried out at a radius of r=2a/3 and both, v and D have been evaluated from experiment by time dependent simulations. The inward drift was estimated to be 0.5 m/s at this radius, this is by a factor of two higher than the neoclassical value used in this paper. The difference might be due to the particle source which has been neglected in Ref. [26].

4.2. *Impurity Transport*

The close connection between energy and particle confinement has been investigated by Fußmann et al. [14]. They have shown that in all regimes with improved energy confinement time metallic impurities tend to accumulate. The enhanced impurity confinement time reflects a reduction of the impurity diffusion coefficient D_I. Titanium laser blow-off experiments have been carried out and from the global analyses of the soft X-ray emission a reduction of the impurity diffusion coefficient from 0.6 to 0.3 m^2/s was found between SOC and IOC regimes, respectively. A simulation of the impurity accumulation during a counter NI heated discharge gave the following result: Using the neoclassical inward drift, the accumulation of copper could be simulated if D_I was reduced from 0.9 to 0.3 m^2/s at the time where the discharge lost the sawteeth. The high neoclassical inward drift was consistent with the observed accumulation of the metallic impurities.

We now come to the aspects of neoclassical impurity transport in sawtooth-free Ohmic discharges. In Fig. 12 the phases of impurity accumulation and saturation of three sawtooth-free discharges with different toroidal field strengths but otherwise identical parameters are analysed using the transport model of Ref. [14]. Since the electron temperatures of these discharges are not very different (see Fig. 14 and 15 for the profiles of the discharges), the soft X-ray intensities are a measure of the metallic impurity concentration (mainly copper). The inward drift is taken according to neoclassical theory and the impurity flux into the plasma is kept the same for all discharges. For the diffusion coefficient we have used the neoclassical term and a constant anomalous contribution: $D_I = D_I^{neo} + D_I^{an}$. With the same D_I^{an} we could simulate accumulation and saturation phases of the three discharges. We have used D_I^{an}=0.12 m^2/s, a value comparable to the diffusion coefficient D of the main plasma species. For the impurities it is of the order of the neoclassical contribution and almost a factor of 3 lower than in the IOC regime.
In order to get an estimate of the influence the B_t dependence of the diffusion coefficient can have on the accumulation level, we rewrite Equations 4b,5a and 5b from Ref. [14] for the diffusion coefficient, D_I, and the inward drift, v_I, in the simplified form:

$$D_I = D_I^{an} + D_I^{PS} + D_I^{cl} = D_I^{an} + (1 + 2q^2) \times D_I^{cl} \tag{3}$$

and

$$v_I = v_I^{PS} + v_I^{cl} \sim (1 + 2q^2) \times D_I^{cl}. \tag{4}$$

In the considered plasmas, the coefficients for copper ions (from the target plates of ASDEX) are given by the anomalous (D_I^{an}), classical (D_I^{cl}) and Pfirsch Schlüter (D_I^{PS}) contributions. At the q=1 surface the degree of accumulation can be written in the form:

$$A_{B_t} \equiv \frac{v_I}{D_I} \sim \frac{3D_I^{cl}}{D_I^{an} + 3D_I^{cl}}. \tag{5}$$

We now use the fact that the analysed discharges have similar profiles and consider only the B_t dependence of D_I^{cl} ($D_I^{cl} \sim B_t^{-2}$). In the analysed profiles $D_I^{an} \cong 1.5(D_I^{PS}+D_I^{cl})$ was used, therefore (from eq. 3: $D_I^{PS}+D_I^{cl}=3D_I^{cl}$) Eq. 5 can be rewritten in the form:

$$A_{B_t} \sim 1/(1 + 1.5B_t^2). \tag{6}$$

The B_t dependence of the neoclassical transport coefficient together with a constant anomalous contribution to the diffusion coefficient explains the difference in the soft X-ray emission for the discharges with B_t=2.18 T and 2.36 T, which have very similar temperature profiles (see Fig. 15): $A_{2.18}/A_{2.36}$=1.15 compared to 1.18 (taken from the soft X-ray radiation levels of the corresponding discharges in Fig. 12). The discharge at B_t=2.0 T has a slightly different central temperature; there we calculate $A_{2.0}/A_{2.18}$=1.16 and measure 1.2 - 1.3. The good agreement may be accidental, but the observed variation of impurity radiation with toroidal field strength is of the right order and direction as predicted by neoclassical theory.
In Doublet III, sawtooth-free discharges were used also for impurity transport studies [9]. Because of large m=1 mode oscillations these discharges were named type O. The

m=1 mode changes the impurity transport behaviour drastically and ends the type O plasma. As discussed in the context of Fig. 8, also at ASDEX m=1 modes can appear during sawtooth-free periods. In Fig. 13 the same discharge as in Fig. 8 is shown again. With the same transport parameters as above we have simulated the soft X-ray emission for this discharge which has quite different plasma parameters. Again the accumulation phase, the turn over and the average trend during the change of line averaged density of the measured soft X-ray signal are well reproduced. This shows that there is no change in the transport behaviour throughout the discharge. The smaller variations in the soft X-ray emission are due to variations in density and electron temperature, but there is no dramatic change when the m=1 mode dies out.

4.3. *Energy Transport*

For the improvement of τ_E found in discharges with peaked density profiles two mechanisms are held to be responsible [5,6]. A common feature is the reduction of the sawtooth activity which accounts for an improvement in the plasma centre. This only gives a contribution to the local improvement, the main effect is speculatively attributed to the steepening of the density gradient in the confinement zone, leading to a suppression of the η_i mode there and to ion energy transport on the level predicted by neoclassical theories.

These arguments also hold for the IOC regime where the linear dependence of τ_E on density extends towards higher values. The loss of the density dependence of τ_E in the SOC regime can be attributed to the anomalous transport mechanisms described above. At low densities IOC and SOC regimes cannot be discriminated. They have the same energy confinement times and, as in the IOC regime, a linear improvement of τ_E with line averaged density. This domain, called LOC regime, can therefore be understood as being governed by a transport mechanism similar to the one in the IOC regime [13] in addition to the effects introduced by a strongly varying Z_{eff} and electron-ion coupling. The anomalous transport mechanisms in the ion channel which are responsible for the degradation in the SOC regime are not as active in this domain or lose their importance as the coupling between ions and electrons weakens towards lower plasma densities. Keeping this in mind, it is not surprising that the global τ_E of sawtooth-free discharges, which have density profiles with even stronger peaking than in IOC plasmas, are only found at the upper margin of the values for the LOC regime.

That the ion energy transport in sawtooth-free discharges is on the neoclassical level can also be seen from Fig. 16. The ion temperature (T_i from active charge exchange) coincides with the band for T_i predicted from neoclassical transport, using radially constant values for Z_{eff} between 1 and 2. The measured profile of Z_{eff} tends more to a value of 2 while the measured ion temperature fits better to the prediction when Z_{eff}=1 was used.

For the energy balance of electrons and ions we use the standard equations for the volume integrated energy fluxes:

$$\Gamma_e(r) = 4\pi^2 R_0 \int_0^r \left(Q_{OH}(r') - Q_{rad}(r') - Q_{ei}(r') - Q_{ion}(r') - \frac{3}{2} \left. \frac{\partial (n_e T_e)}{\partial t} \right|_{r'} \right) r' dr' \quad (7)$$

$$\Gamma_i(r) = 4\pi^2 R_0 \int_0^r \left(-Q_{cx}(r') + Q_{ei}(r') - Q_{ion}(r') - \frac{3}{2} \left. \frac{\partial (n_i T_i)}{\partial t} \right|_{r'} \right) r' dr'. \quad (8)$$

The energy transported by electrons (Γ_e) and ions (Γ_i) across a flux surface are given by integrals over the sources and sinks inside the flux surface. Ohmic heating (Q_{OH}), charge exchange (Q_{cx}), neutral ionization (Q_{ion}), impurity radiation profiles from Abel-inverted bolometer measurements (Q_{rad}) and electron ion coupling (Q_{ei}) are taken into account. The neutral particle density is calculated using the AURORA Monte Carlo code [27].
The fluxes are then interpreted by an ansatz for diffusive transport which includes the convective losses caused by a net particle flux as calculated by Eq. 1.

$$\Gamma_e(r) = \frac{5}{2}\Gamma_n(r)T_e(r) - \chi_e \nabla T_e(r) S(r), \quad (9)$$

$$\Gamma_i(r) = \frac{5}{2}\Gamma_n(r)T_i(r) - \chi_i \nabla T_i(r) S(r). \quad (10)$$

If the temperatures are measured, the fluxes are equivalent to experimental data and Eqs. 9 and 10 are used to estimate the transport coefficients χ_e and χ_i. A different approach is to start, as it was done for the calculated ion temperature profile of Fig. 16, from a prediction for the ion energy transport coefficient and to evaluate the ion temperature profile from Eqs. 10, 8. For Fig. 16, the Z_{eff} dependent neoclassical ion heat conductivity from Ref. [25] has been used.
For a direct comparison of the energy transport in discharges with and without sawteeth, we analyse a discharge similar to the sawtooth-free one of Fig. 1 in the Ohmic phases before and after NI heating. NI introduces sawteeth to the OH phase following the beam pulse. From what was said above, it is justified to use neoclassical transport for the ion channel in the early sawtooth-free and the late sawtoothing phase. Then, the ion transport contributes with about 30% to the total energy transport.
The measured electron temperature and density profiles in the two phases are represented by the full lines in Figs. 14 and 15. In Fig. 17 the contributions to the electron transport are given. The enhanced radiative loss in the plasma centre during the sawtooth-free phase of the discharge is the main difference to the late phase with sawteeth. The minor differences in the electron-ion exchange term are due to variations in the Z_{eff} ($Z_{eff} \cong 1.9$ and 2.2, with and without sawteeth, respectively) and density profiles.
Apparently, a reduction of the sawtooth energy transport does not lead to higher T_e values in the plasma centre. Instead strong radiation takes over the role of an important loss term which is surprisingly well restricted to the interior of the q=1 surface ($r_{q=1}$=11 cm), the region where the sawtooth previously contributed most to the energy transport. As a result one finds a strong reduction of the thermal electron diffusivity, as shown in Fig. 18. This is, however, misleading, since in the χ_e of the discharge with sawteeth the contribution from the sawtooth transport is contained.
An estimate from a simple sawtooth model using the sawtooth amplitude on the electron temperature and the repetition time [6] shows that the reduction in χ_e cannot be explained by the vanishing of the sawteeth alone. The energy which is, according to this model, normally transported by the sawteeth across the q=1 surface is only about

25% of the radiated power in the interior of this region in the sawtooth-free case. In the plasma centre one ends up with very small values ($\chi_e \ll 1$ m^2/s) for the electron heat conductivity. In the outer region of the plasma the electron energy transport coefficients for discharges with and without sawteeth coincide within the error bars of the calculation. Without sawteeth, both D and χ_e are observed to drop within the region bound typically by the radius of the q=1 surface, D and χ_e are both lower than the values obtained with sawteeth even after the mere convective losses from sawtooth activity has been subtracted.

Although the ion energy transport only plays a minor role in low density Ohmic discharges, from neutron emission rates some improvement can be deduced when sawteeth disappear. In the discharge above the neutron emission rate drops by a factor of 2 when the sawteeth are active. Ion density profile effects can only explain 50% of this difference. The remaining difference can be explained by using, when predicting the ion temperature for the phase with sawteeth, in addition to the neoclassical ion energy transport model the simple sawtooth model cited above. This enhances the ion energy transport in the plasma centre and lower ion temperatures and neutron rates are calculated. Even though the error bars are large on this kind of investigation it gives additional confidence in the assumption that ion energy transport in the LOC is governed by neoclassical processes.

Finally we consider the η_i mode [28] which could be responsible for the degradation in confinement at higher plasma densities with broader density profiles. In Fig. 19 we plot the radial dependence of η_i (ion density over ion temperature gradient length) for the sawtooth-free discharge of Figs. 16 and 8, which served as an example that there is not much room for anomalous ion energy transport in sawtooth-free discharges. In the region important for the confinement, the value of η_i, calculated from the actual ion density profile, exceeds the critical value. This mode should then contribute appreciably to the ion energy transport. This is in contradiction to the results of Fig. 16.

5. Summary

A comparison of ASDEX discharges with and without sawteeth showed the existence of two stable modes in Ohmically heated tokamak plasmas. The sawtooth-free discharge is a realisation of a quiescent plasma with its "natural", peaked density profile. The sawtooth instability is responsible for the quasi-steady state of the normally observed discharges with flatter density profiles.

The energy confinement time of sawtooth-free discharges is superior to that in the LOC and SOC regimes. This is consistent with the observation that the peaking of the density profile leads to an improvement of energy confinement time. There are two possibilities for a density profile peaking: In the IOC regime, the peaking is triggered from the plasma edge while in sawtooth-free discharges it is a process bound to the centre. The first case is more efficient for the improvement of energy confinement time and the improvement in the sawtooth-free discharges is therefore less important than in these discharges.

The stabilization of the sawtooth instability can appear at central q values below 1 and can be possibly attributed to the steep density gradient at the q=1 surface. The

behaviour of the central MHD activity is in agreement with the q profiles as deduced from current density calculations with neoclassical resistivity.

Using neoclassical inward drift velocities for plasma particles and impurities one can explain the electron density profiles and the impurity accumulation with the same anomalous transport coefficient of 0.1 m^2/s. In the case of the accumulating copper ions this is of the order of the prediction of neoclassical theory. A strong m=1 mode, which can coexist with sawtooth-free phases, does not change the impurity transport behaviour. The particle diffusion coefficient does not depend on q_a.

At low densities, in the LOC regime, the ion heat conductivity is on the level of the neoclassical transport coefficient irrespective, whether sawteeth are active or not. A stabilization of the sawtooth instability improves only the transport coefficient in the plasma centre. Also for the thermal electron diffusion coefficient only in the centre an improvement is seen. Because of the high radiation level in the centre of sawtooth-free discharges a value of $\chi_e \ll 1$ m^2/s is deduced from the energy balance. Outside the sawtooth mixing radius the diffusion coefficients coincide within the uncertainties of the calculations. It seems to be a general behaviour of a tokamak plasma that its electron heat diffusivity responses the net heating power to be transported. χ_e increases with heating power but it decreases in cases where impurity radiation reduces the thermal power flow. The electron temperature profile only loses its rigidity and the temperature starts decreasing if the radiation losses rather exactly balance the power input.

In conclusion: Stationary sawtooth-free discharges in the LOC regime allowed for analyses of a peaked density plasma. Current density, particle and impurity inward drift velocities and ion heat conductivity are consistent with the predictions from neoclassical theories. The anomalous contributions to the particle and impurity diffusion coefficient are small and of the same order of magnitude. The electron heat conductivity remains anomalous, but very small values were found in the centre of the discharge were impurity radiation almost balances the Ohmic heating power so that only a small amount of energy has to be transported by the electrons. Contrarily to the expectations, the reduction of the power flux in the centre does not lead to a flattening of the temperature gradient but to a reduction in the electron heat conductivity.

Acknowledgement: The authors wish to thank K. Lackner for helpful discussions and for pointing to Ref. [23].

References

[1] SÖLDNER, F. X., MÜLLER, E. R., WAGNER, F., BOSCH, H. S., EBERHAGEN, A., et al., Phys. Rev. Lett. **61** (1988) 1105.

[2] GRUBER, O., KAUFMANN, M., LACKNER, K., LANG, R. S., MERTENS, V., et al., Comparison of confinement in hydrogen versus deuterium in multi-pellet fuelled OH discharges in ASDEX, in *Proc. of the* 15^{th} *Europ. Conf. on Controlled Fusion and Plasma Heating, Dubrovnik*, pages 27–30, 1988.

[3] GEHRE, O., GRUBER, O., MURMANN, H. D., ROBERTS, D. E., WAGNER, F., et al., Phys. Rev. Lett. **60** (1988) 1502.

[4] ASDEX team, Nucl. Fusion **29** (1989) 1959.

[5] GRUBER, O., WAGNER, F., KAUFMANN, M., LACKNER, K., MURMANN, H., et al., Influence of density profile shape on plasma transport in ASDEX, in *Proc. of the* 15^{th} *Europ. Conf. on Controlled Fusion and Plasma Heating, Dubrovnik*, pages 23–26, 1988.

[6] STROTH, U., FAHRBACH, H.-U., HERRMANN, W., and MAYER, H.-M., Nucl. Fusion **29** (1989) 761.

[7] CAMPBELL, D. J., START, D. F. H., WESSON, J. A., BARTLETT, D. V., BHATNAGAR, V. P., et al., Phys. Rev. Lett. **60** (1988) 2148.

[8] CHRISTIANSEN, J. P., CORDEY, J. G., and MUIR, D. G., Nucl. Fusion **29** (1989) 1505.

[9] JAHNS, G. L., EJIMA, S., GROEBNER, R. J., BROOKS, N. H., FISHER, R. K., et al., Nucl. Fusion **22** (1982) 1049.

[10] WAGNER, F., SÖLDNER, F. X., STEINMETZ, K., BECKER, G., BOSCH, H.-S., et al., Plasma Phys. Controlled Fusion **28** (1986) 1225.

[11] SCHNEIDER, U., POSCHENRIEDER, W., BESSENRODT-WEBERPALS, M., HOFMANN, J., KALLENBACH, A., et al., Boronization of ASDEX, in *Proc. of the* 9^{th} *International Conf. on Plasma Surface Interactions in Controlled Fusion Devices, Bournemouth*, 1990.

[12] RÖHR, H., STEUER, K.-H., MURMANN, H., and MEISEL, D., Periodische Vielkanal-Thomson-Streuung, IPP Report III/121, Max-Planck-Institut für Plasmaphysik, Garching, F.R.G., 1987.

[13] BESSENRODT-WEBERPALS, M., McCORMICK, K., SÖLDNER, F. X., WAGNER, F., BOSCH, H.-S., et al., Nucl. Fusion **31** (1991) 155.

[14] FUSSMANN, G., HOFMANN, J., JANESCHITZ, G., KRIEGER, K., MÜLLER, E. R., et al., J. Nucl. Mater. **162** (1989) 14.

[15] NOLTE, R., FUSSMANN, G., and GRUBER, O., Sawtooth activity during impurity accumulation in ASDEX, in *Proc. of the* 16^{th} *Europ. Conf. on Controlled Fusion and Plasma Heating, Venice*, pages 549–552, 1989.

[16] ENGELHARDT, W., KLÜBER, O., LACKNER, K., and SESNIC, S., Disruptive instability caused by impurity accumulation, in *Proceedings of the IAEA Symposium on Current Disruptions in Toroidal Devices*, 1979.

[17] SÖLDNER, F. X., McCORMICK, K., ECKHARTT, D., KORNHERR, M., LEUTERER, F., et al., Phys. Rev. Lett. **57** (1986) 1137.

[18] McCORMICK, K., SÖLDNER, F. X., ECKHARTT, D., LEUTERER, F., MURMANN, H., et al., Phys. Rev. Lett. **58** (1987) 491.

[19] CHU, T. K., BELL, R., BERNABEI, S., CAVALLO, A., GUHARAY, S., et al., Nucl. Fusion **26** (1986) 666.

[20] SÖLDNER, F. X., BARTIROMO, R., BERNABEI, S., HARVEY, R. W., LEUTERER, F., et al., Profile control with lower hyprid waves on ASDEX, in *Proc. of the* 17^{th} *Europ. Conf. on Controlled Fusion and Plasma Heating, Amsterdam*, pages 1323–1326, 1990.

[21] SÖLDNER, F. X. and private communication.

[22] HIRSHMAN, S. P., HAWRYLUK, R. J., and BIRGE, B., Nucl. Fusion **17** (1977) 611.

[23] COPPI, B., ENGLADE, S., MIGLIUOLO, S., PORCELLI, F., and SUGIYAMA, L., Ingition physics processes and compact experiments, in *Plasma Physics and Controlled Fusion Research (Proc.* 11^{th} *Int. Conf., Kyoto, 1986), Vol. 3 IAEA, Vienna*, pages 397–406, 1987.

[24] PORCELLI, F., CAMPBELL, D., DIACHENKO, W. D., ERIKSSON, L.-G., JACQUINOT, J., et al., Sawtooth stabilisation by fast ions: Comparison between theory and experiments, in *Proc. of the* 17^{th} *Europ. Conf. on Controlled Fusion and Plasma Heating, Amsterdam*, pages 327–330, 1990.

[25] CHANG, C. S. and HINTON, F. L., Phys. Fluids **29** (1986) 3314.

[26] MERTENS, V., BÜCHEL, K., GRUBER, O., KAUFMANN, M., KORNHERR, M., et al., Particle transport and sawtooth activity in pellet-fuelled ASDEX L-mode plasmas, in *Proc. of the* 16^{th} *Europ. Conf. on Controlled Fusion and Plasma Heating, Venice*, pages 183–186, 1989.

[27] HUGHES, M. H. and POST, D. E., J. Comput. Phys. **28** (1978) 43.

[28] LEE, G. S. and DIAMOND, P. H., Phys. Fluids **29** (1986) 3291.

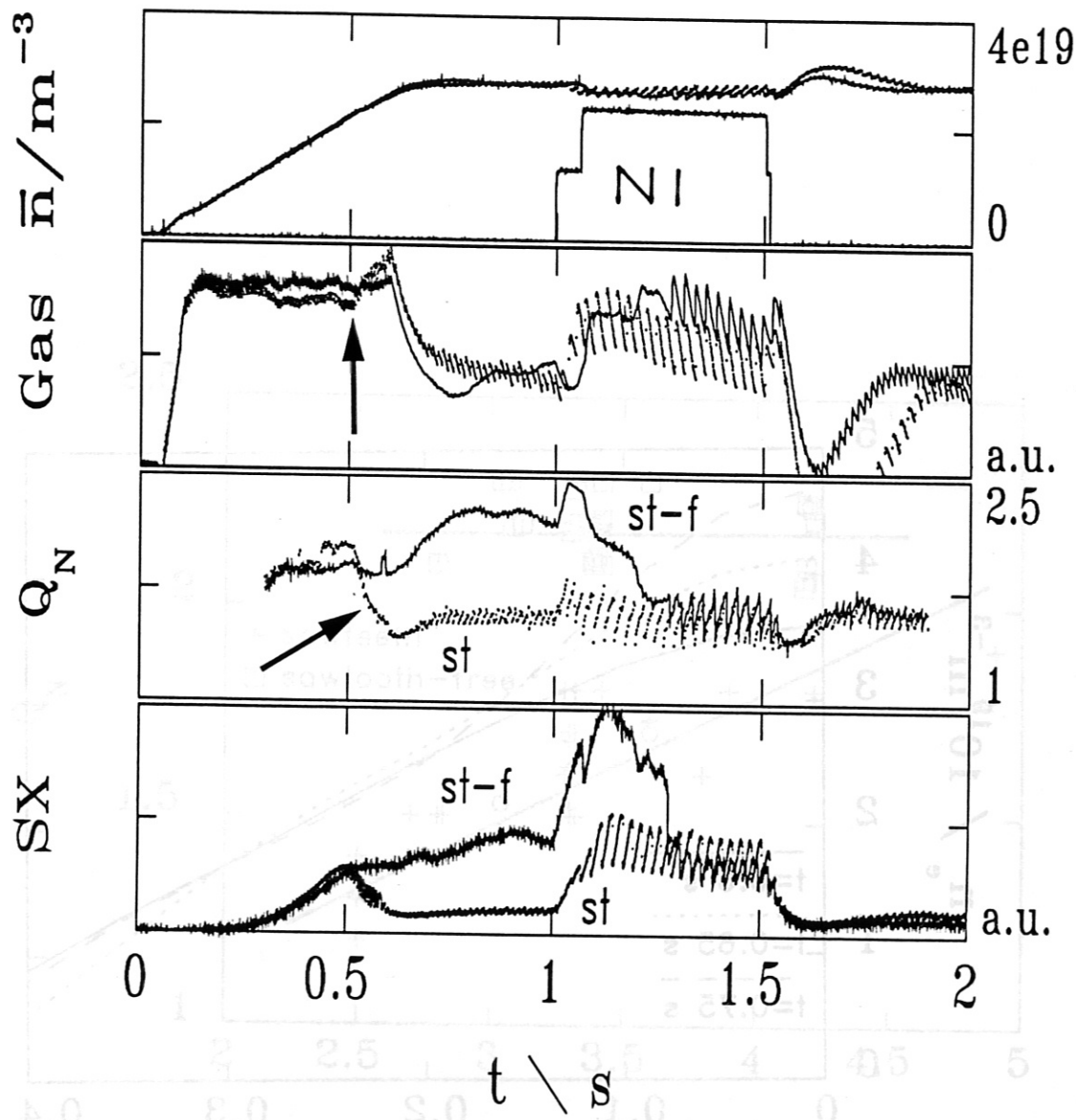

Figure 1: Temporal evolution of discharges with (st, dotted line) and without (st-f, full line) sawteeth: Line averaged density, external gas flux to the plasma, density peaking factor and soft X-ray radiation from a central chord. The sawtooth-free phase is terminated at 1.3 s during the NI-heating interval. Both are deuterium discharges with I_P=320 kA and $\bar{n}_e = 2.8 \times 10^{19} \mathrm{m}^{-3}$. The toroidal field strengths are B_t=2.0 T (q_a=3.05) and 1.8 T (q_a=2.8) in the st-f and st discharges, respectively.

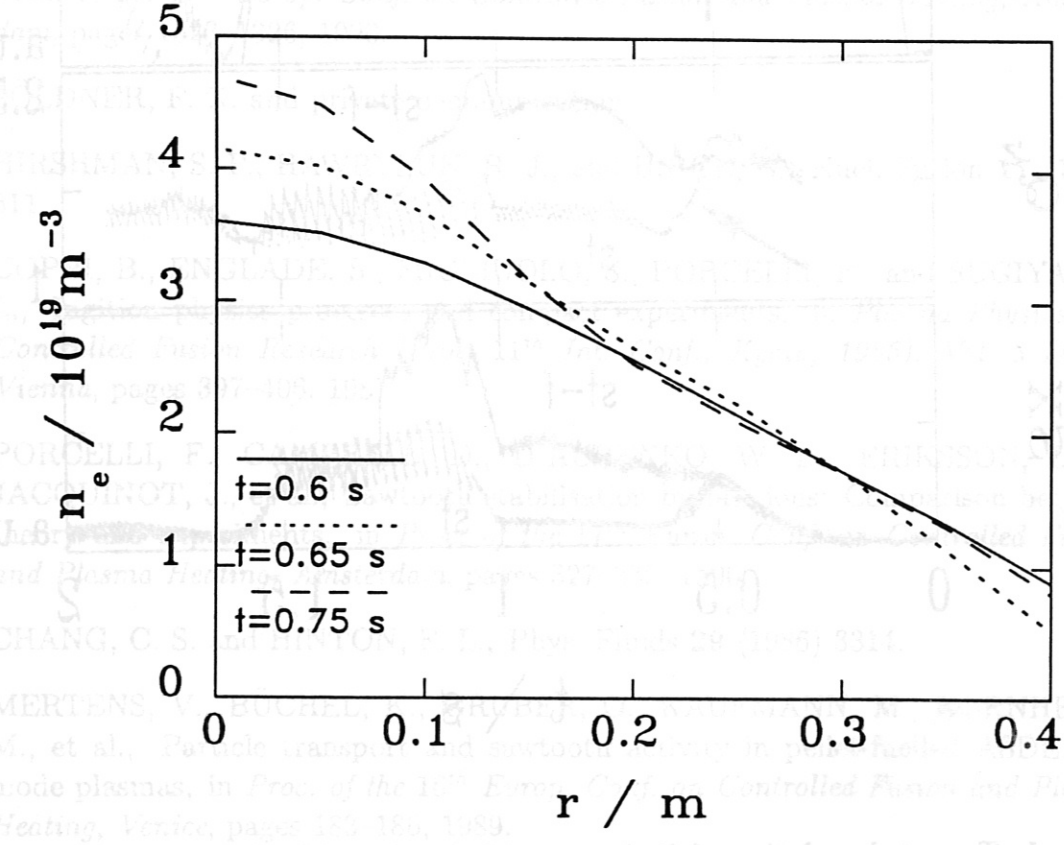

Figure 2: Electron density profiles of the sawtooth-free discharge of Fig. 1 at 3 time points before, during and after the steep rise in the density peaking factor.

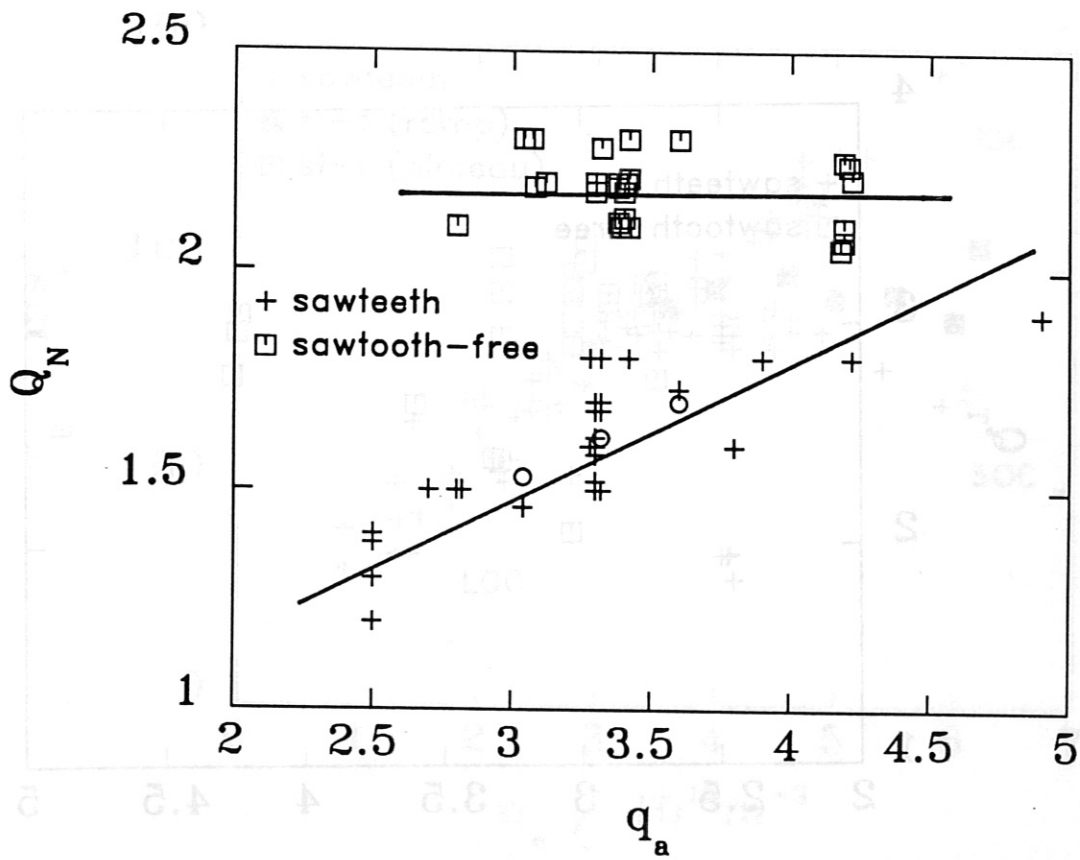

Figure 3: Central to volume averaged electron density as a function of q_a for discharges with and without sawteeth. The lines are drawn in order to guide the eye. The circles represent values obtained from profiles of sawtooth-free discharges where it was assumed that the sawteeth basically flatten the density profile in the region bound by the q=1 surface (see text).

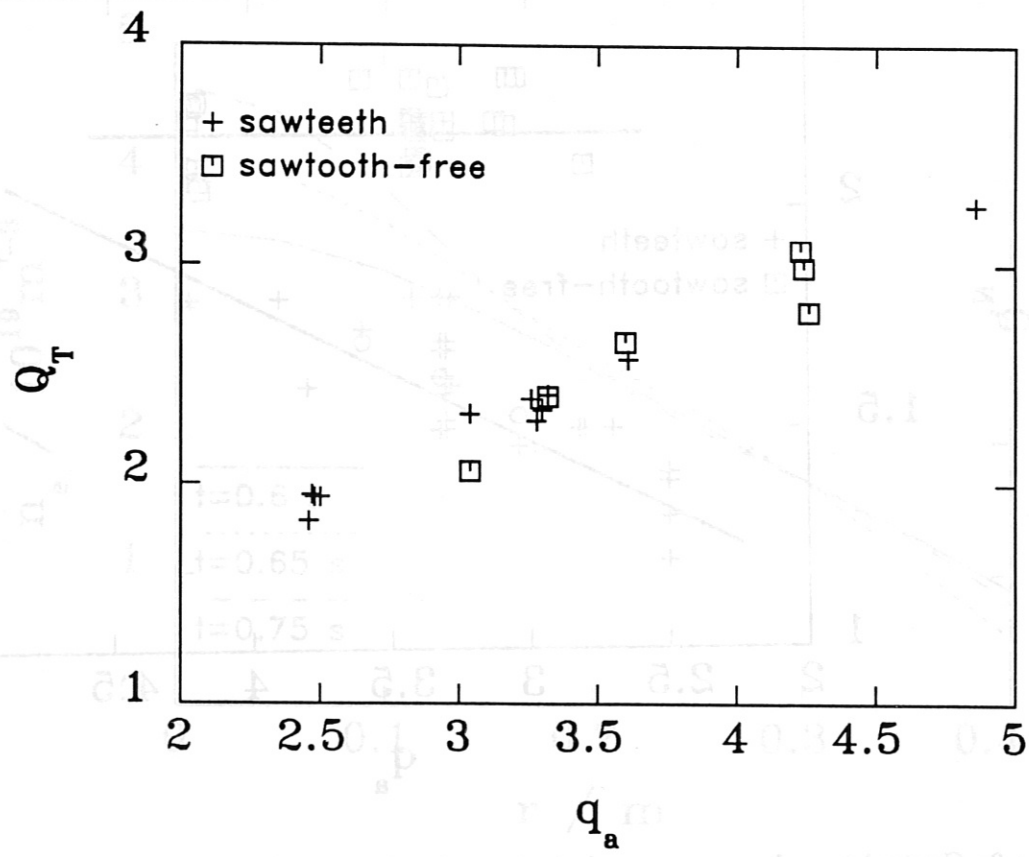

Figure 4: Central to volume averaged electron temperature (Q_T) as function of q_a for discharges with and without sawteeth.

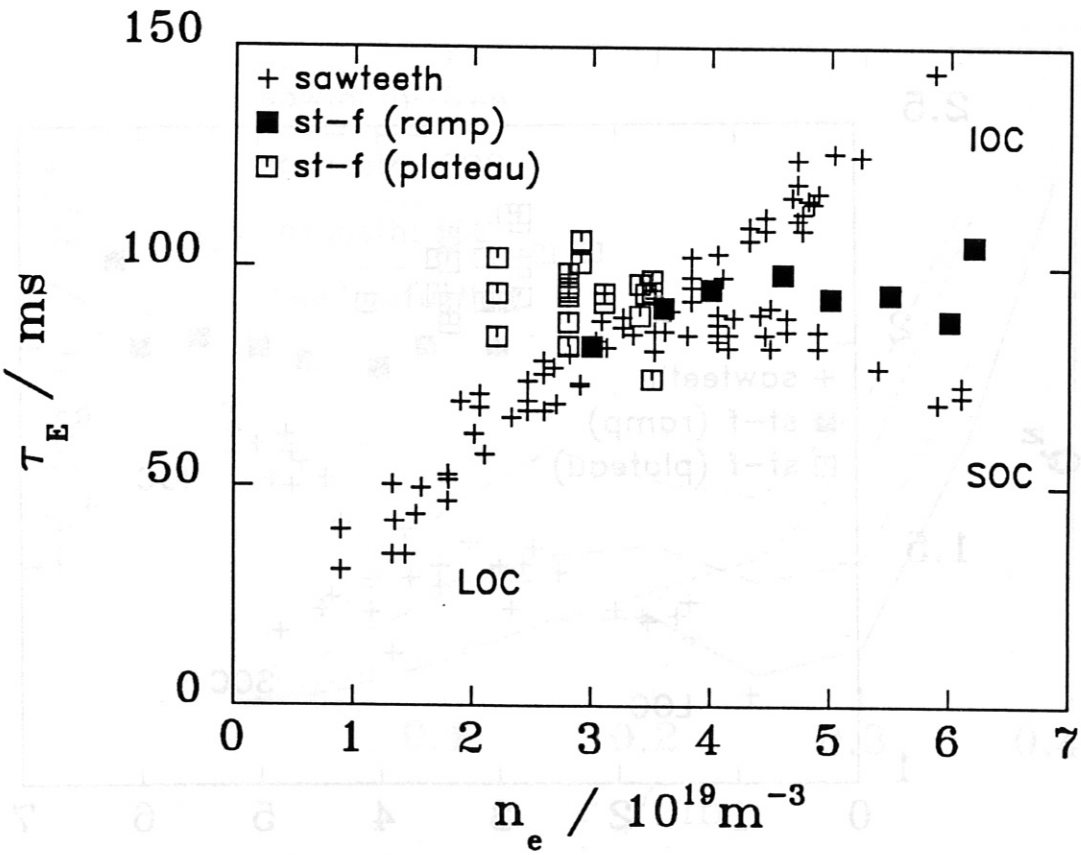

Figure 5: Diamagnetic global energy confinement time as a function of line averaged density in the Linear (LOC), Saturated (SOC) and Improved (IOC) Ohmic Confinement regimes for discharges with and without sawteeth. For the sawtooth-free discharges at high densities (full squares only) the density has been ramped up linearly. The discharges with sawteeth are at q_a=2.75.

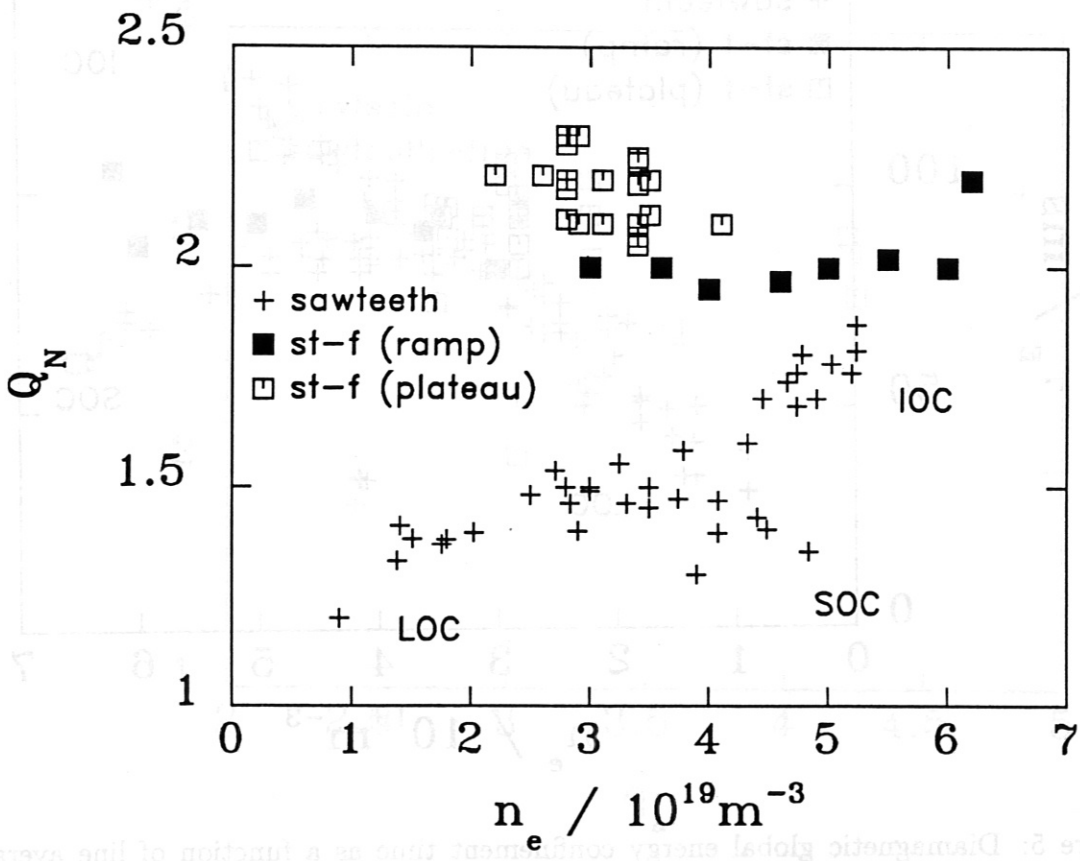

Figure 6: The same as Fig. 5 but for the density peaking factor.

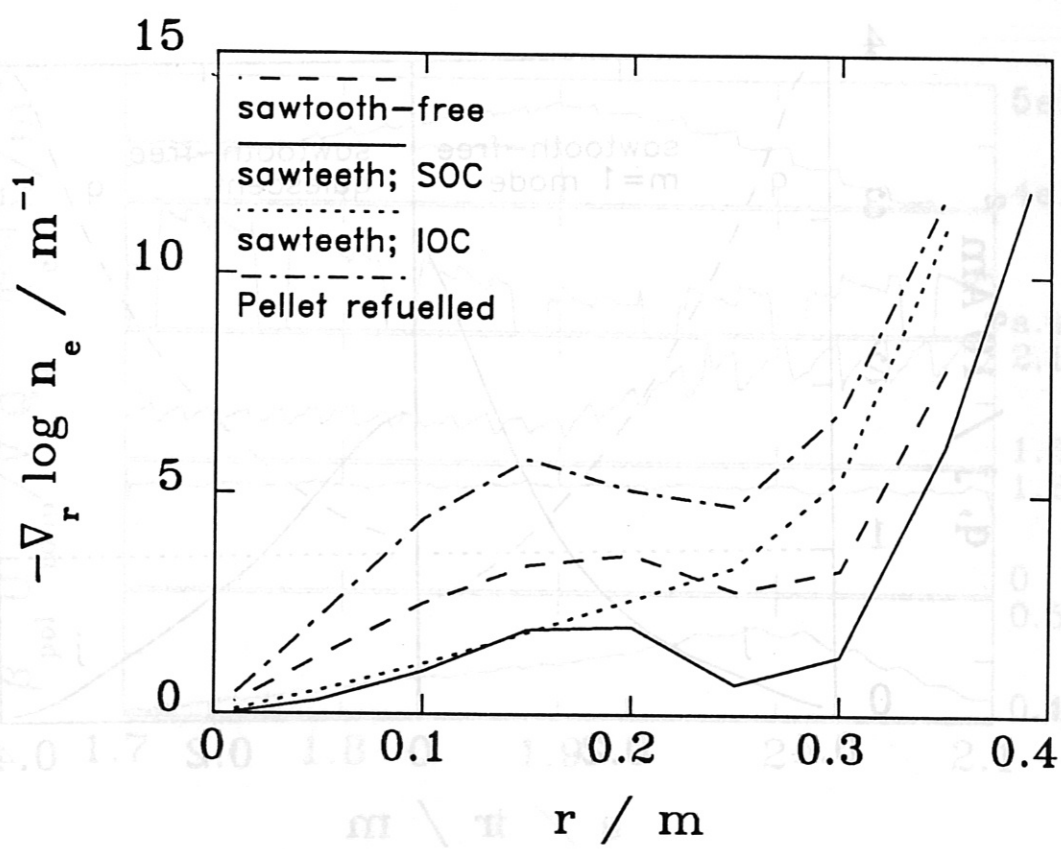

Figure 7: Local electron density scale lengths for discharges in different OH regimes: Sawtooth-free ($\bar{n}_e$ =5.6 × 10^{19}m^{-3}, q_a=3.3), sawtoothing with gaspuff ($\bar{n}_e$ = 7.3×10^{19}m^{-3}, q_a=2.7), IOC ($\bar{n}_e$ = 5.0×10^{19}m^{-3}, q_a=2.8) and pellet refuelled ($\bar{n}_e$ = 6.6×10^{19}m^{-3}, q_a=2.8). The pellet refuelled discharge has the strongest peaked density profile. The density profile from the sawtooth-free discharge is only in the plasma centre and the IOC profile only at the plasma edge steeper than the profile of the SOC discharge.

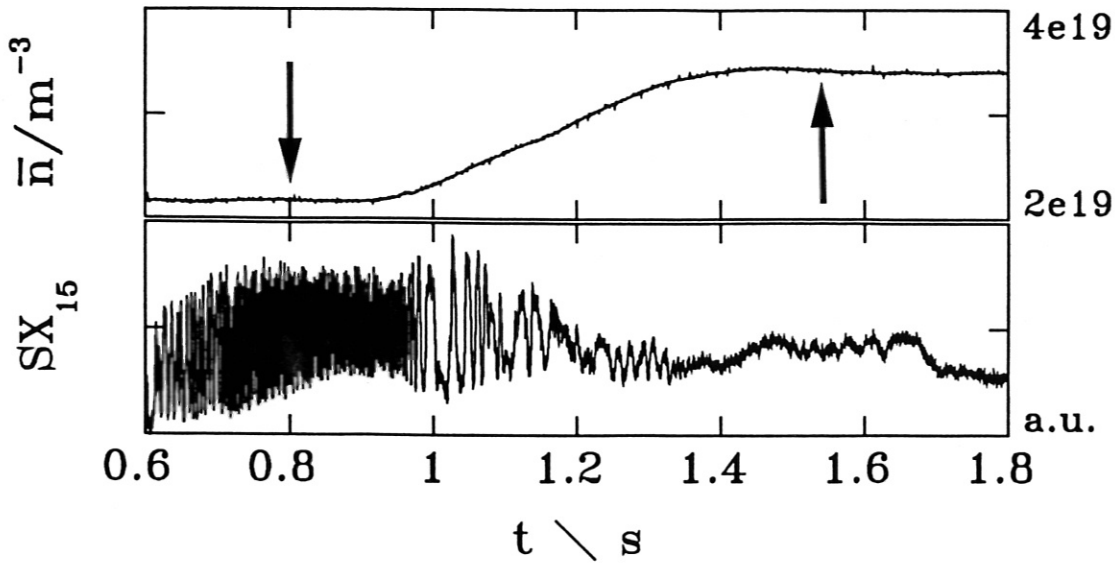

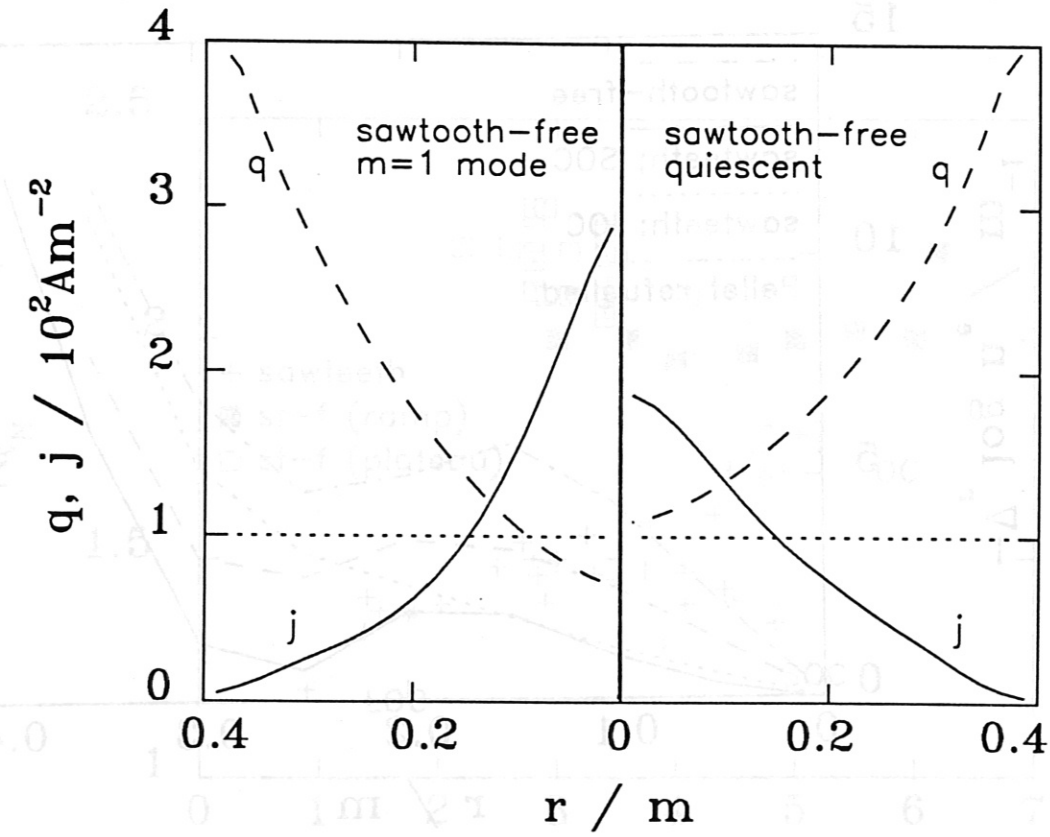

Figure 8: A sawtooth-free Ohmic discharge at q_a=4.2 and I_P=250 kA. Upper part: line averaged density with two plateaus and a non-central chord (r=5cm) of the soft X-ray camera array, showing an m=1 mode at the low density and a quiescent phase at the high density. Bottom: Results from a neoclassical current density calculation and the deduced q profiles for the time points indicated by the arrows.

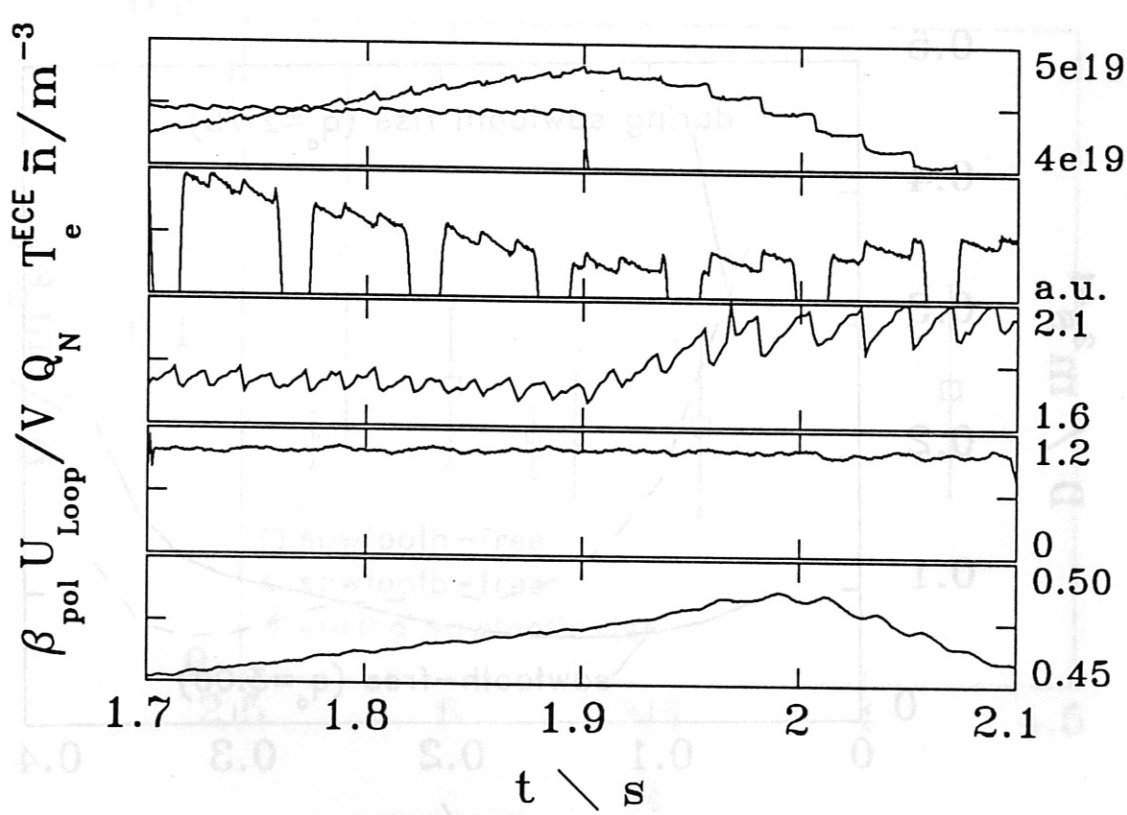

Figure 9: The influence of the external gas flux into the plasma on the sawtooth behaviour. Line averaged density, non-central ECE electron temperature, density peaking factor, loop voltage and the diamagnetic β poloidal signal are displayed. The Ohmically heated discharge was with I_P=317 kA and q_a=3.3. The ECE signal is periodically interrupted to monitor the base line.

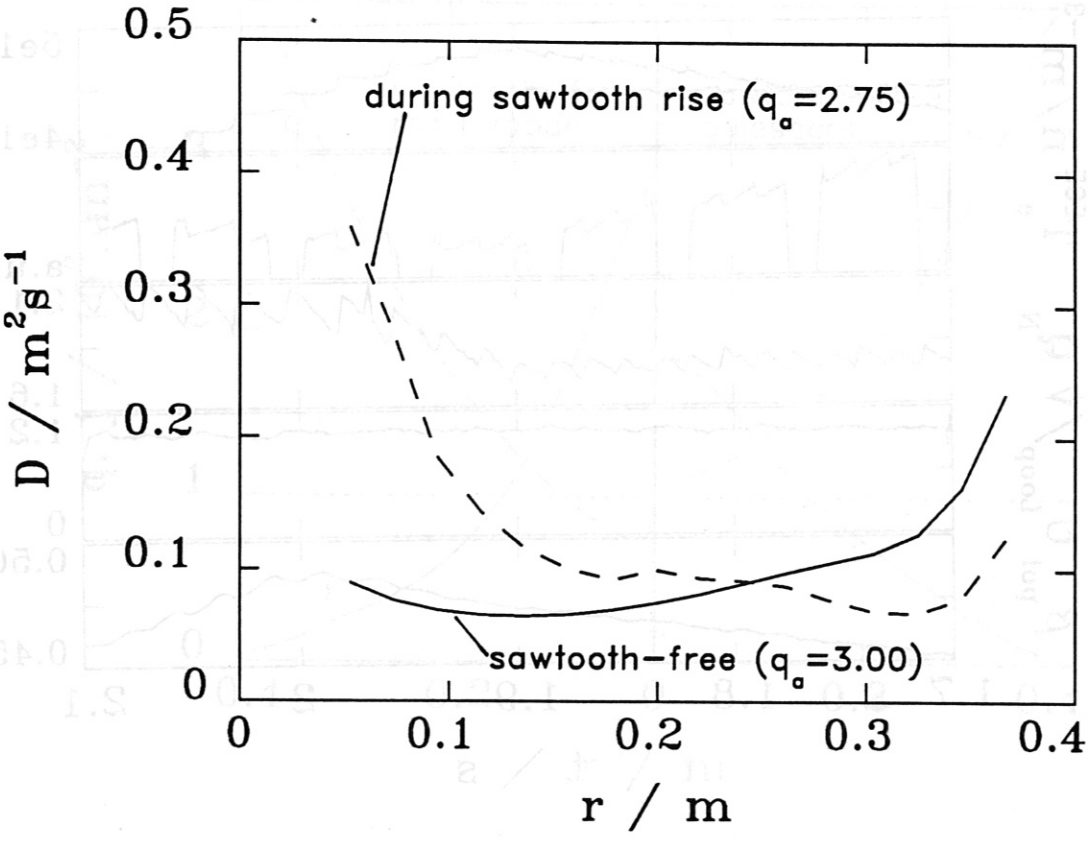

Figure 10: Particle diffusion coefficient for a sawtooth-free discharge and during the rise of a sawtooth. Realistic particle sources and a neoclassical Ware pinch are included in the calculation.

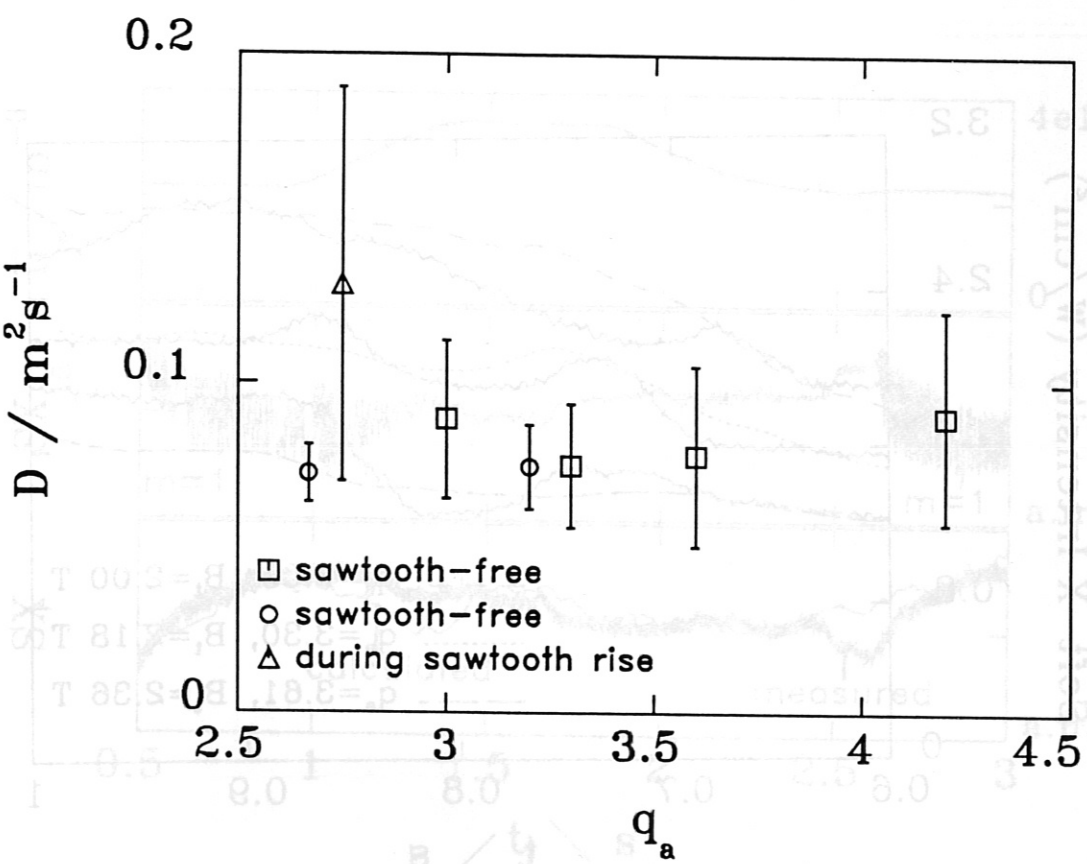

Figure 11: Particle diffusion coefficients averaged between r=a/4 and r=3a/4 (a is the minor plasma radius) for sawtooth-free discharges and a discharge during a sawtooth rise phase as a function of the edge safety factor. The error bars give the variation of D in the region of averaging. Circles: B_t=2.18 T; I_P=318 and 378 kA; squares: I_P=318 kA, B_t= 2.0, 2.17 and 2.36 T. $\bar{n}_e$=3 10^{19}m^{-3} in all discharges.

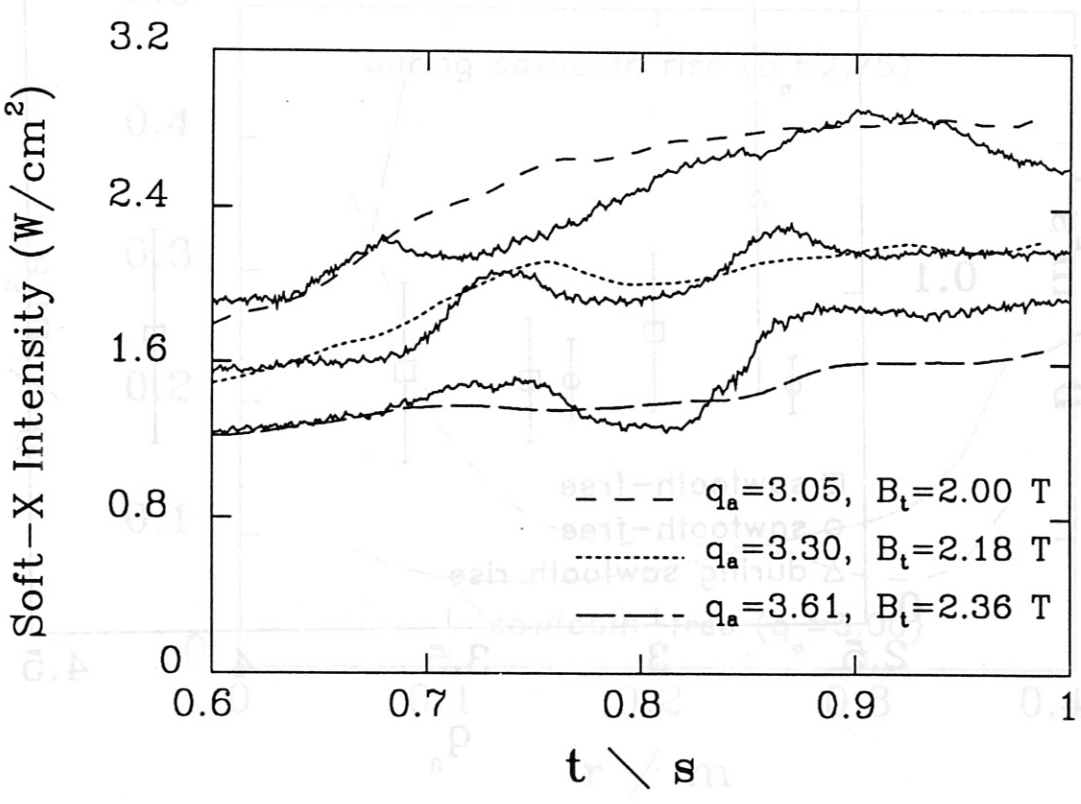

Figure 12: Measured and calculated soft X-ray intensities of three sawtooth-free discharges at different toroidal field strengths. The calculations have been performed assuming copper as the dominant impurity, neoclassical inward drift and a diffusion coefficient with neoclassical and additional anomalous contributions of 0.1 m^2/s.

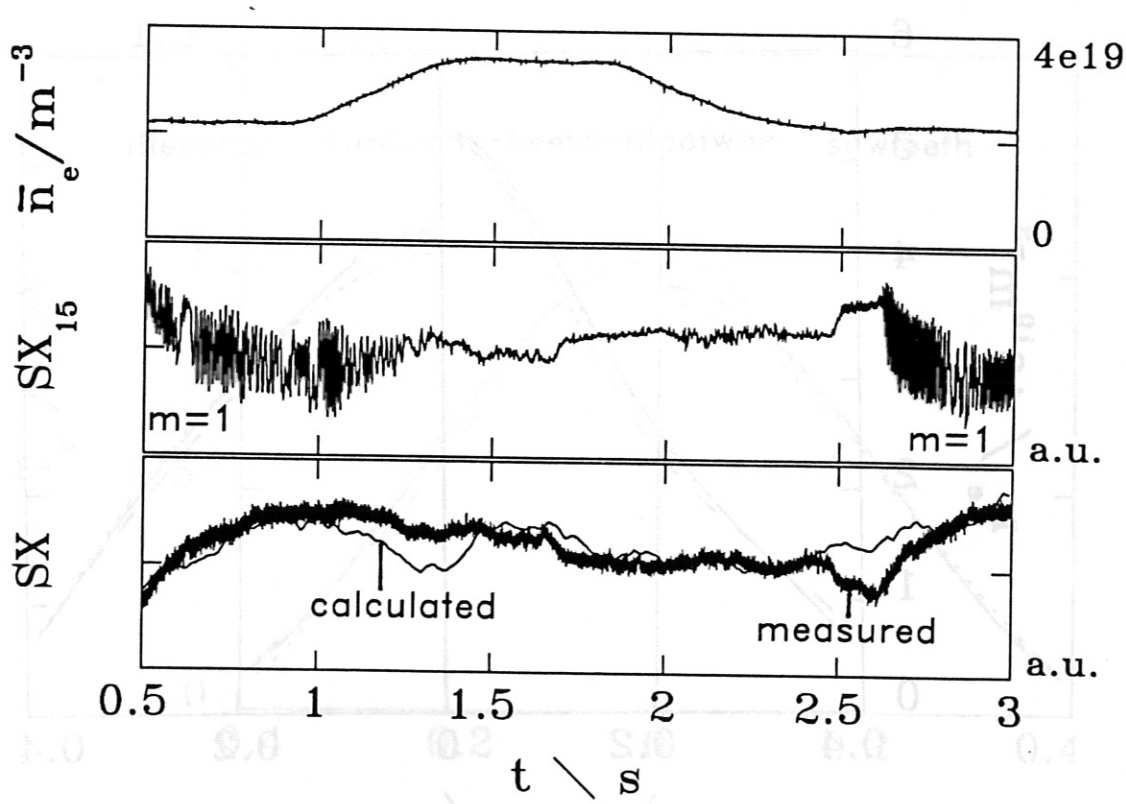

Figure 13: Line averaged density with two plateaus and a non-central chord (r=5cm) of the soft X-ray camera array showing and m=1 mode at the lower density and a quiescent phase at the higher density. Lower part: Measured and calculated soft X-ray intensities of a central chord calculated with the same impurity transport parameters as in Fig. 12.

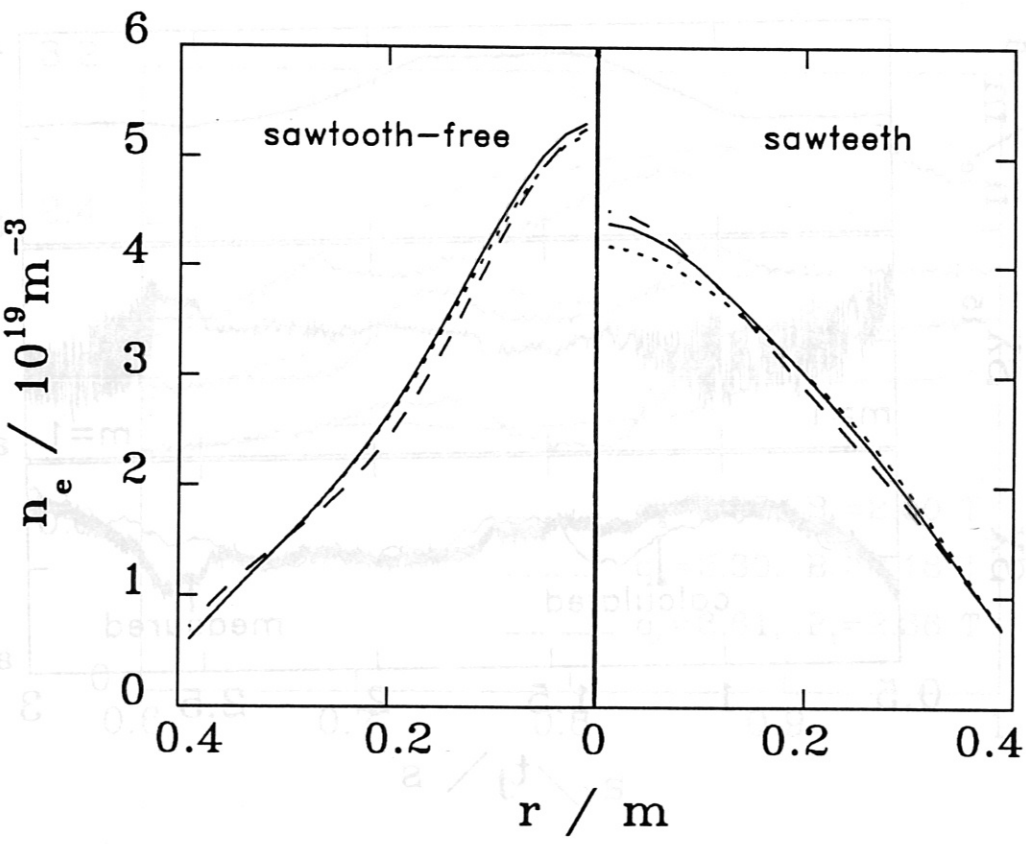

Figure 14: Density profiles of discharges with and without sawteeth at different toroidal field strengths: q_a=3.0 (dotted), q_a=3.3 (full) and q_a=3.6 (dashed line).

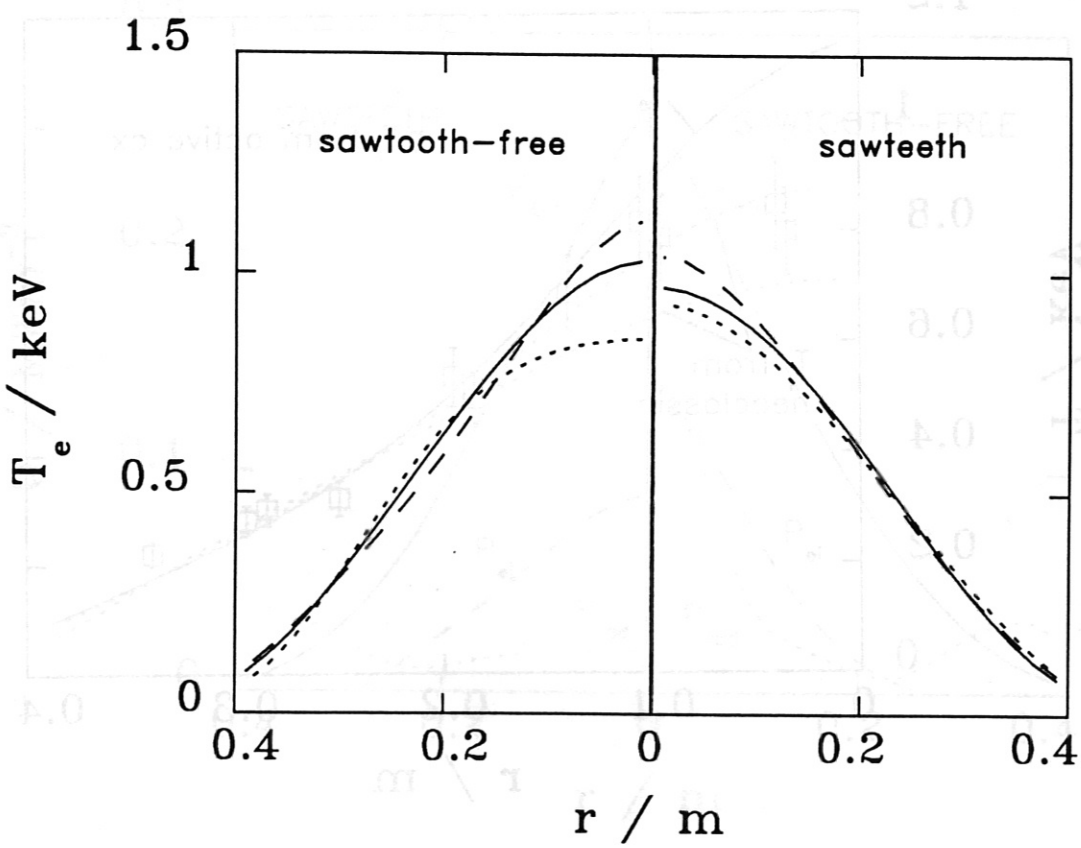

Figure 15: Temperature profiles of discharges with and without sawteeth at different toroidal field strengths: q_a=3.0 (dotted), q_a=3.3 (full) and q_a=3.6 (dashed line).

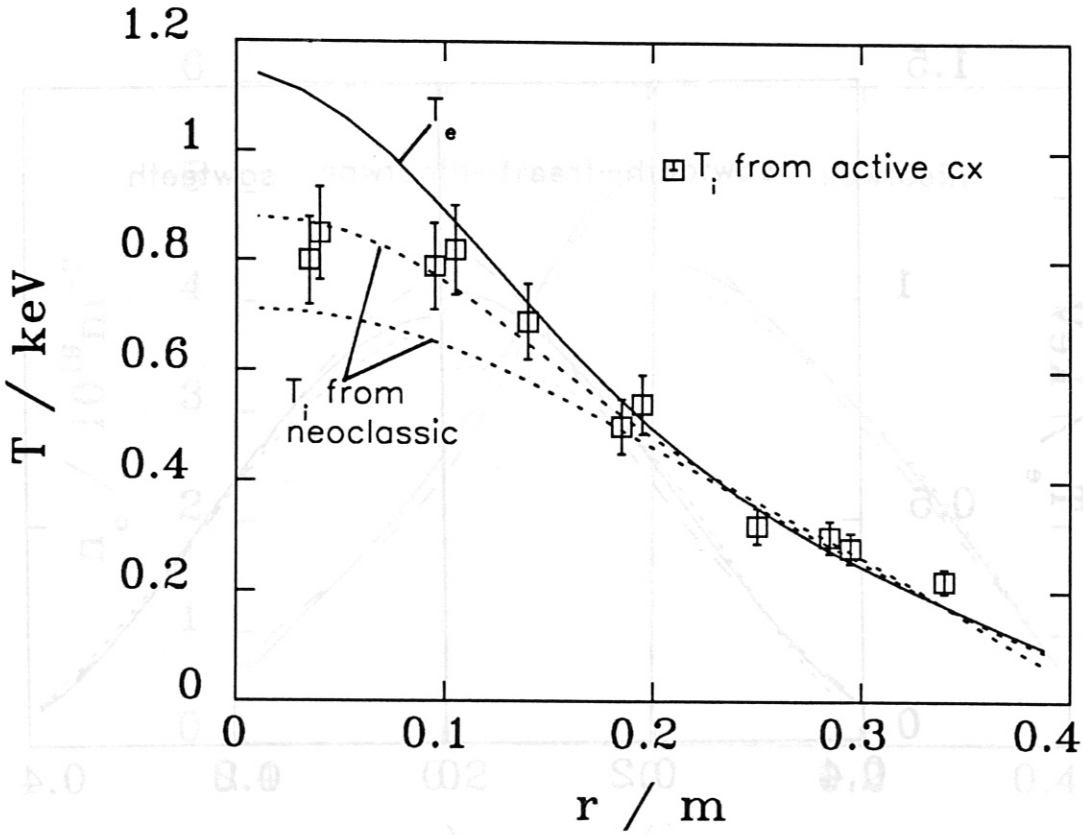

Figure 16: Electron and ion temperatures at 0.8 s of the discharge in Fig.8. The dashed line represents predictions from neoclassical theory with constant Z_{eff} of 1 (upper curve) and 2 (lower curve). The squares are results from an active beam neutral particle analyser.

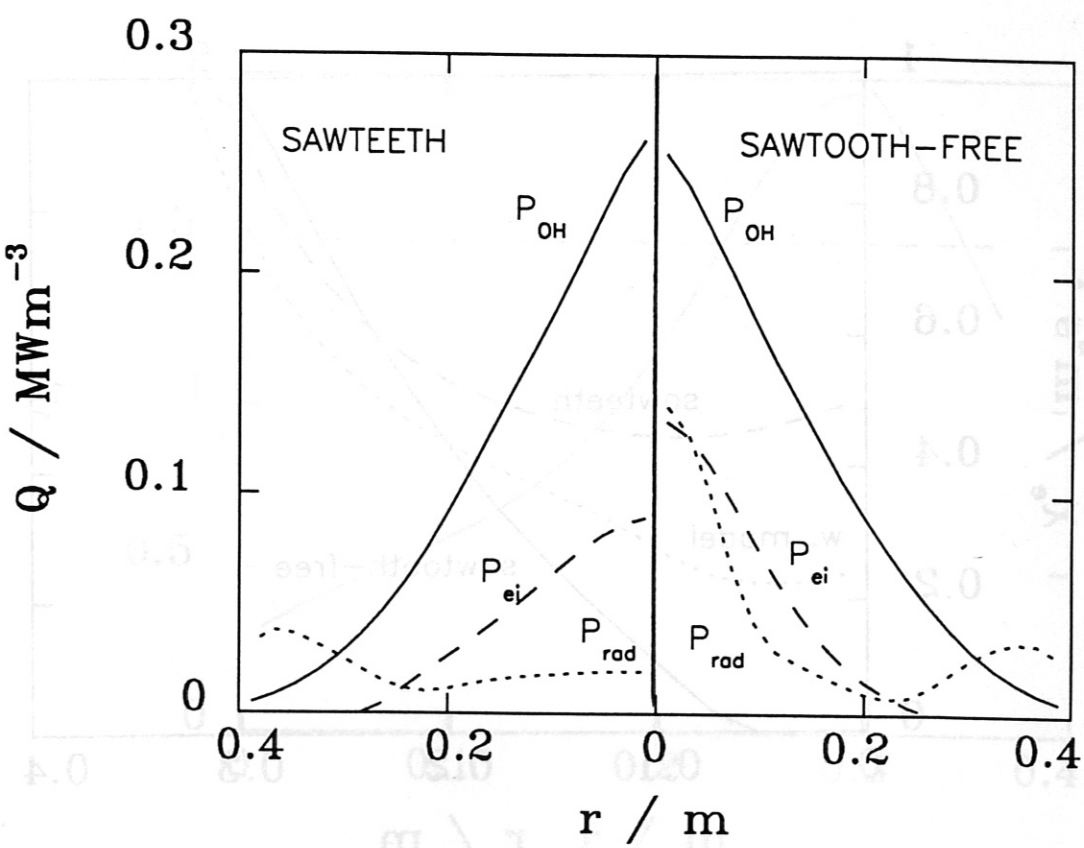

Figure 17: Electron power balance for discharges with (left) and without (right) sawteeth. Ohmic (full), radiation (dotted) and electron ion exchange (dashed) contributions are plotted. The plasma parameters are: I_P=320 kA and $\bar{n}_e$=2.8×10^{19}m^{-3}.

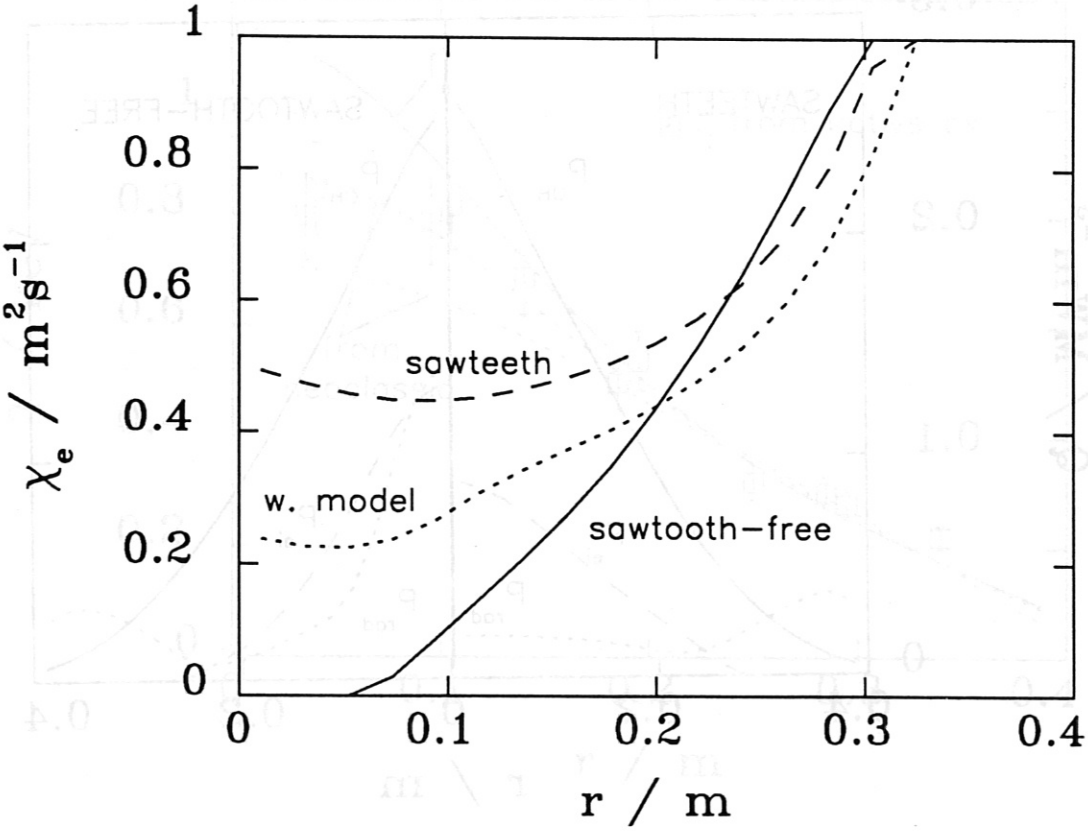

Figure 18: Electron heat diffusivities for the discharge of Fig.17. The dotted line gives the diffusivity for the phase with sawteeth if a sawtooth model is included in the calculation.

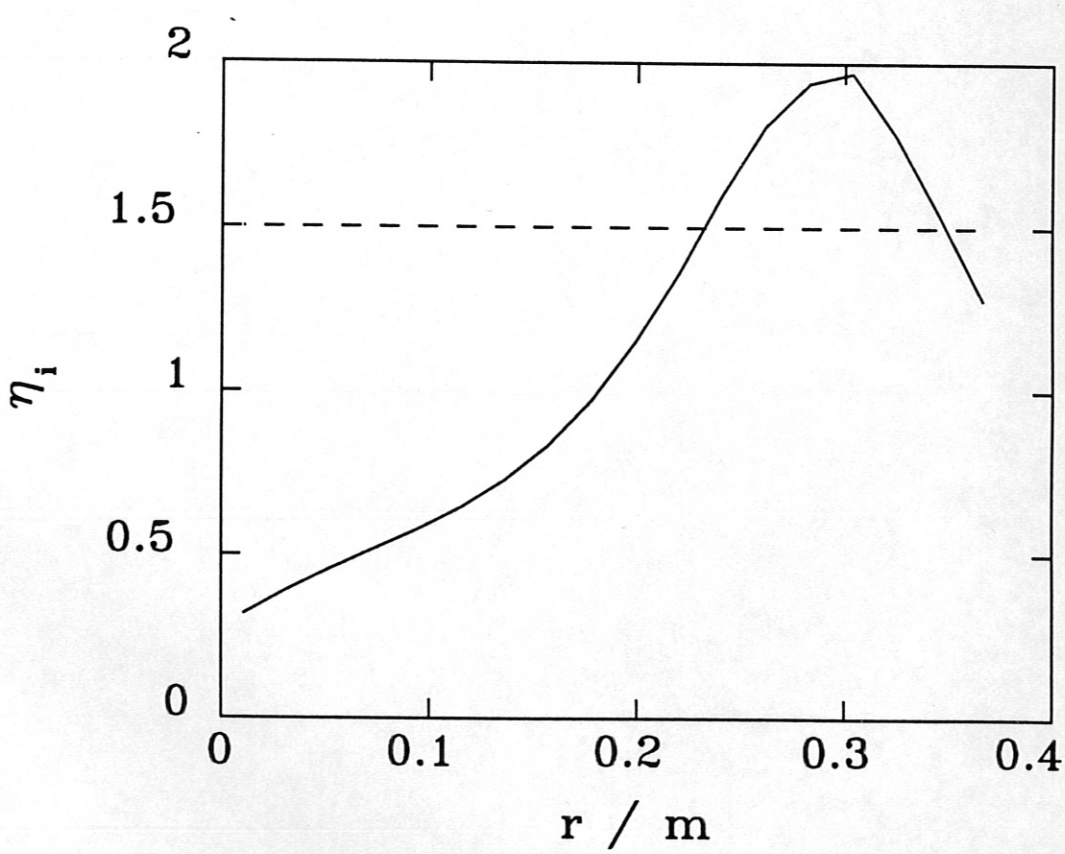

Figure 19: η_i for the sawtooth-free phase of the discharge in Fig.16 as a function of minor radius. The critical value for destabilizing the η_i mode is indicated by the dashed line.